Journal of Control Engineering Practice (*CEP'03*)
vol. 11, num. 12, pp 1413 – 1421, December 2003.

# Comparison of structured light and stereovision sensors for new Airbag Generations*

S. Boverie†, M. Devy‡, F.Lerasle‡¶
† Siemens VDO Automotive SAS, BP 1149, 31036 Toulouse Cedex 1 (France)
‡ LAAS-CNRS, 7 avenue Colonel Roche 31077 Toulouse Cedex
¶ Université Paul Sabatier, 118 route de Narbonne, 31062 Toulouse Cedex

August 25, 2006

**Abstract**

Providing new generations of airbags with reliable information about the vehicle inner space occupancy in order to minimize inappropriate inflation is a real challenge. Within this paper two techniques to rebuilt the 3D cockpit scene, are presented; beside the well-known stereoscopic vision principles, 3D reconstruction based on matricial sensor combined with an infrared structured light emitter is described. From the 3D points acquired by these sensors a 3D description of the seat area is built, pertinent attributes are extracted, and using a previously learnt data base, the current seat situation is identified amongst the learnt situations (empty seat, baby seat in normal or rear position, occupant, ...). First promising results are depicted.

## 1 Introduction

These last years a special effort has been focused on the improvement of passive safety both by car manufacturers and suppliers all over the world. Frontal airbags for the driver and the passenger are now mounted in almost every new car. In brief lateral airbags will be massively installed. The most part of these airbag systems are operating in open loop conditions. That means that whenever an impact is detected, the airbag is automatically inflated without any feedback from the seat occupant nature. This operating mode has caused some dramatic situations, for example: babies installed on a baby seat in rear position thrown to the back of the vehicle when airbag inflates, passengers in "out of position" situation who are injured by the airbag...

*This project was supported and funded by the PREDIT II program of the french Ministry of National Education and Research.

In US, 97th statistics show that airbags saved about 1600 lives. It is also acknowledged that they killed 32 childrens and 20 small adults. New generations of airbags need to be more "intelligent" to provide appropriate inflations with regard to the vehicle inner space situation and thus to minimize the injury risk. The improvement of this function requires the introduction of new sensors to provide reliable information about the cockpit occupancy such as passenger nature, occupant morphology, occupant volumic distribution to detect "out of position" situations of the passenger (figure 1). This information will then be used by airbag Electronic Control Units (ECUs) in order to take the appropriate decisions (figure 2). Classical systems fuse heterogeneous physical measures provided by optical, pressure, capacity, thermical or weight sensors placed between the seat and the dashboard, for example the PDS from BMW, the IROPS from Siemens VDO or the Delphi's systems. Data fusion of such sensors increases of course the system reliability or performance but these devices remain inadequate to give pertinent informations such as the passenger posture for example. More sophisticated techniques have been explored: time of flight sensor and well-known stereoscopic vision. A time of flight sensor [1] is based on a NIR laser diode and a CMOS camera with an ultra short integration time; the intensity measured at the CMOS sensor depends on the distance and the surface reflexion. A recent improvement of such systems consists in determining the light propagation time by multiple double short time integration [11]. Advantages of this system are its cost, its insentivity to backlight and its high-integrated possibilities while a major drawback concerns the need of the short illumination time and the good synchronization between the camera shutter and the light source.


Figure 1: Scenarii for occupant detection

Stereoscopic vision is based on the principle that depth information can be computed by triangulation from two images with a common area in their field of view. For many years, many developments have led to mature 3D perception methods [10, 6]. P Faber et al in [4] use a dense stereoscopic method to detect the passenger presence. The basic principle consists in looking for the passenger head. Krumm et al in [7] are looking for three classes, rear facing baby seat, empty seat and other situations. They show: (1) a first approach using monocular vision and ACP on an image base in order to find a minimal dimension of the space in which it is possible to separate the

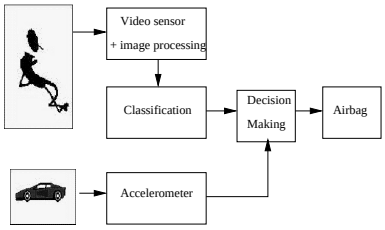


Figure 2: System architecture

three classes, (2) a second approach takes advantage of the same classification methods but with data provided by a stereoscopic sensor. Results look less good but more stable in relation with light disturbances.

In our project, two different solutions have been developped. Beside the passive stereoscopic sensor, an active 3D vision system has been developped, based on a CCD camera combined with an IR structured ligth emitter. From one or another system, 3D reconstruction is reached and attribute vectors are then extracted and allow to identify the current seat situation among the learnt ones illustrated in figure 1.

These two vision based methods will be presented and discussed in this paper, with respect to several criteria: density of the acquired depth images, acquisition speed, mechanical and safety constraints... The first promising results with these different technologies will be presented.

# 2 Structured light based approach

## 2.1 Generalities

This approach developed by Siemens VDO Automotive in collaboration with LAAS-CNRS and ONERA-DOTA is concerned with 3D active vision system based on a matricial sensor combined with an infrared structured light emitter. This principle is currently used in other application fields as robotics, architecture... [2, 12, 13]. A light pattern is projected onto the scene, the 2D deformation of this pattern in the image plane due to the objects contained in the scene is analyzed. Then once the sensor is calibrated, triangulation techniques allow to give 3D data on the observed scene. The latest step of this process is the extraction of specific characteristics from the 3D reconstruction and then the classification. This technique is usually applied with supervised environmental conditions (light control...), low real time constraints and no light power restrictions.

The approach is original in the sense that the system has to cope with specific automotive constraints and to present a good robustness with respect to an uncontrolled light disturbances and back-light. These constraints has required the development of specific measurement devices and algorithms in order to classify all the most current situations regarding occupant safety.

## 2.2 Sensor presentation

The efficiency of such a system depends on some characteristics like the resolution of the sensor and light emitter, the gap between the light emitter and the sensor, the calibration accuracy, the radiance of the beams, its location in the cockpit... The gap between the light emitter and the sensor must be large enough to allow 2 $cm$ accuracy on 3D points located at 1 $m$ from the camera. A too large gap will lead to mounting problems and to occluded beams. A 6 $cm$ gap has issued good results. The light emitter is composed of a laser diode

(830 $nm$ wavelength), a Damman diffraction grid that split the original beam into several beams and a concave planar lens to spread the illumination on a conic field of $90° \times 70°$.

The light emitter resolution is quite critical in order to determine if there is a person or an object on the seat and to distinguish head, arms... from a passenger. Current developments have been performed with a $11 \times 11$ array of beams that demonstrate a good compromise between 3D reconstruction accuracy and calculation time. Another prototype has been designed with $19 \times 16$ beams to have a meaningful reconstruction for demo-car (figure 3-(a)). Each laser beam $D_f$ is labelled by its row and column position in the array (figure 3-(b)).

In order to brighten the dots on the image, the radiance of each beam should be maximized by optimizing the output power (limited by the eye safety requirements) and narrowing the beam diameter. The maximal output power is function of the wavelength of the emitted light and of the operating modes of the illuminator. As an example for an illuminator wavelength of 850 $nm$, operating in a pulse mode of 1ms duration every 10 $ms$, the maximum permissible power considering, non intentional vision is 0.78 $mW$ (Standard IEC 825-1). Pulse duration of 100 $\mu s$ would increase the permissible power by a factor 2.

Image acquisition is carried out using a single short focal length CCD camera with a 2.6 $mm$ lens providing an field of view of $130° \times 100°$. The off line calibration step determines the parameters corresponding to the well-known perspective projection camera model, taking into account intra and inter sensor/illuminator and lens characteristics [3]. At first, the camera calibration process consists in estimating in one global step both the intrinsic and distortion parameters from matchings between a set of points defined on a planar calibration target and their projections on the image plane. To reduce the measurement errors, the computation of the parameters is done with multiple pose of this target.

Then another calibration process is required to identify the laser beams equation parameters in the camera coordinate system. It uses multiple views of the same calibration target on which the lasers beams are projected (figure 3-(c)).

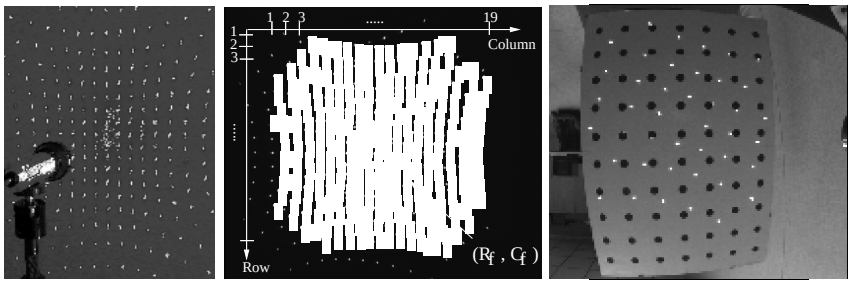


(a) (b) (c)

Figure 3: (a) Laser beams, (b) associated labels, (c) calibration target

The camera/illuminator device is located in the overhead console position which appears to be the most efficient position since it provides the best overview of the passenger seat even if it has two drawbacks. The first one is the need of a very wide angle of sight of the illuminator/camera ($> 90°$). The second one is that the compactness requirement gets critical which could lead to mount the ECU in a distant location.

## 2.3 3D reconstruction and classification

The occupant detection methodology can be decomposed in a 3D reconstruction process and then a classification one, both detailled hereafter. The 3D reconstruction process requires itself two steps. The **first step** concerns the extraction of light dots, intersections of laser beams with the image plane, by the way of conventional image processing techniques that have to deal with problems like light disturbances (shadows, direct sunlight...), passenger movement, surfaces with low reflexivity, specular reflections...

The **second step** is related to the dot labeling, e.g. the search of matchings between the light dots and the laser beams. The labeling process is based on the sequential application of the following constraints:

**Epipolar constraint:** For each dot $i$, after distortion correction, and each beam $D_f$, the distance in the image between the dot and the $D_f$ projection (noted $D_{f_{proj}}$) is calculated. A matching $(i, f)$ is discarded if the distance $d(i, f)$ exceeds a certain tolerance, generally three or four pixels in experiments. Figure 4 shows light beams projections in the image plane. The different crosses represent the extracted light dots over time. Although the beams projections are very close to each other, thanks to this first constraints, the number of candidate beams $D_f$ to correspond to a light dot $i$ is drastically reduced (about 95%).

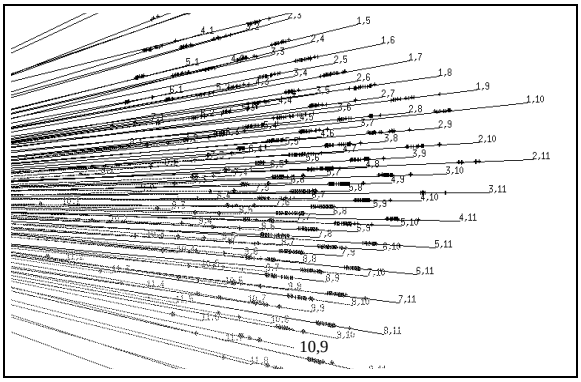


Figure 4: Image dots positions and associated projected beams

**Depth constraints:** for cockpit occupancy reconstruction, the triangulation must yield to 3D points whose depth lies within the range $[0, 1.5\ m]$. A matching

$(i, f)$ is discarded, if the depth of the resulting reconstructed 3D point, exceeds this threshold.

**Topological constraints:** the two following constraints allow to evaluate the matching confidence:

(a) uniqueness: each laser beam must be imaged with, at most, one light dot. So, a beam label can be associated to at most one dot and vice versa.

(b) order: this constraint implying pairs of light dots, is applied only if their two labels belong to the same column or row in the array of beams (figure 3-(b)). Given two light dots $p_i = (u_i, v_i)^T$ and $p_j = (u_j, v_j)^T$, two labels $f$ (column $C_f$, row $R_f$) and $g$ (column $C_g$, row $R_g$), the order constraint is:

*if $R_f = R_g$ (resp. $C_f = C_g$) then (i,f) and (j,g) are consistent* $\Leftrightarrow$ *$(C_f, C_g)$ (resp. $(R_f, R_g)$) and $(v_i, v_j)$ (resp. $(u_i, u_j)$) are in the same order.*

To apply these constraints, three different optimization techniques have been evaluated maximal cliques, continuous relaxation and discrete relaxation [9]. This last one has shown the better compromise between speed and matching performances. Its principle can be summarized as follows: a first pass, defined by epipolar and depth constraints, exhibits trustworthy and ambiguous labellings, depending on whether a dot $i$ matches a unique beam $f_0$ or may be associated with several ones. Topological constraints are next checked for the remaining ambiguous matchings [8]. The discrete iterative relaxation process is set up so as to eliminate the ambiguous matchings that are incompatible with confident ones regarding some uniqueness and order relationships. Consequently, the total number of confident matchings increases iteratively.

From the labelling process results and the off-line calibration phase, 3D coordinates can be computed. From the 3D points, the 3D shape is then represented by a triangular mesh (figure 7). Referring to the final decision related with airbag inflation, the different scenarii described in figure 1 can be grouped and reduced to a simpler set represented in figure 5.

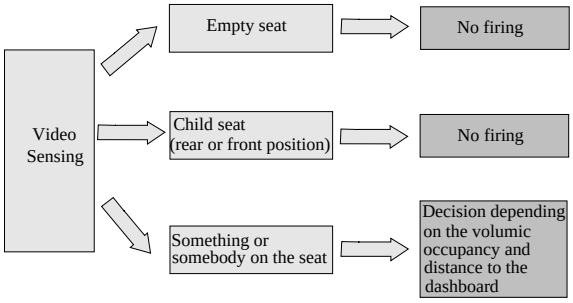


Figure 5: The different scenarii and associated airbags operating conditions

The classification method is also based on a hierarchical process. The **first level** consists in detecting one of the three occupant categories: empty seat, baby seat, "something" on the seat. It is based, on the one hand, on the analysis of the motion of the objects located within the observed scene and, on the other hand, on the extraction of specific attributes related to each occupancy class and

computed in some analysis areas defined in the vehicle longitudinal projection plane. The 3D reconstructed points are simply projected onto this particular plane to have a kind of scene profile characteristic of the occupancy class (figure 8). The analysis areas correspond to three horizontally-oriented stripes in the longitudinal plane and are located as follows : one which envelops the seat sitting and the two other located just above the seat sitting. The classification is made by the method of the $K$ nearest neighbours, from the results of the attributes learnt in a database built from images acquired on the different seat occupancy classes.

In case of "something" is detected on the seat, a **second processing level** estimates the position of the occupant with respect to two operating zones of the airbag. This very simple technique is based on the analysis of the number of light dots in each zone. These zones are defined according to an emerging normalization about the critical volume close to the dashboard (figure 6): the Critical Out Of Position (COOP) and Out Of Position (OOP) volumes. The only criterion for the definition of these zones, consists in the distance to the dashboard (invariant w.r.t. the seat position). Finally, this information is then fused in order to provide a final decision to the airbag ECU.

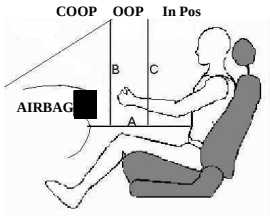

Figure 6: OOP and COOP zones

## 2.4 Results

The different algorithms have been implemented in C code on a 400 MHz PC. 3D reconstruction is performed each 50 $ms$ for a $11 \times 11$ array of beams. Figure 7 shows two examples of reconstruction provided with the $19 \times 16$ array. The right sub-figures represent the triangular meshes generated from the 3D points. The results show that the system is able to give a very good approximation of the volumetric distribution of the occupancy within the observed scene. In addition a very good estimation of the distances between the dashboard and the occupant is achieved ($\pm$ 2 $cm$).

The classification even if it is based on very simple principles gives promising results. The tests that have been performed in real situations have proved that it is able to make the distinction between the most important occupancy classes listed before. In addition this technique allows to make the distinction between the different dashboard proximity situations. In a further step, the analysis of the dynamic evolution of the situation along an image sequence, will lead to an improvement of the classification robustness.

Figure 8 shows two scenarii examples and their projections in the longitudinal plane. In the first case, some reconstructed points are close to the airbag, so the airbag must not fire. In the second case, the airbag firing is compatible with the analyzed situation.

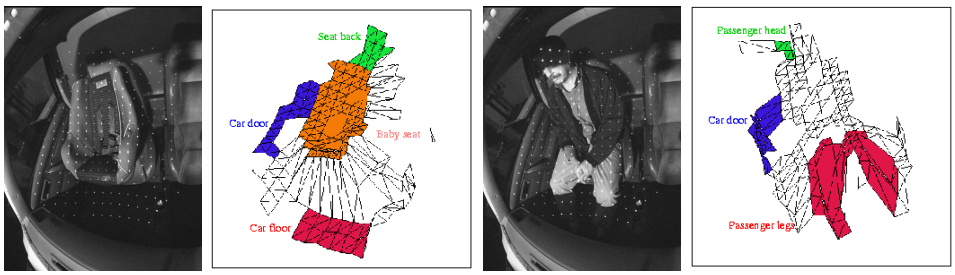


(a) (b)

Figure 7: 3D reconstruction of scenarii: (a) empty baby seat, (b) passenger on the seat

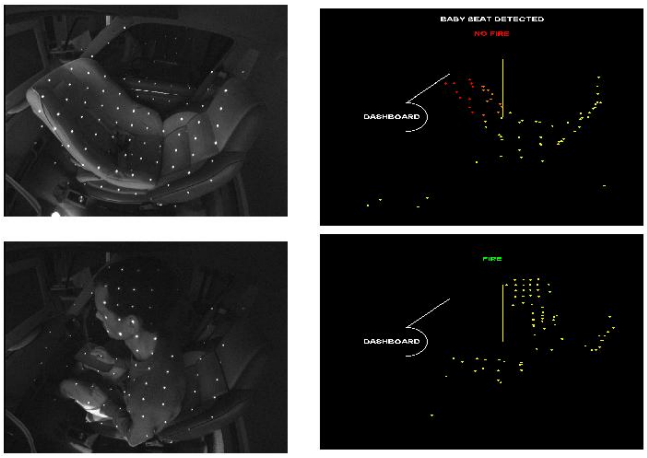


(a) (b)

Figure 8: (a) Original images, (b) reconstruction projection in the vehicle longitudinal plane and associated airbags operating conditions

# 3 Stereovision based approach

Concerning the stereoscopic vision, developments take profit of well-known principles and aim to adapt them to the constrained automotive context: real time performances, dense and accurate reconstruction, low cost technology...

## 3.1 3D acquisition from stereovision

The pixel-based stereo algorithm aims to match pixels between left and right images [5] acquired by the stereo cameras. The stereovision process includes several steps. An off-line calibration determines the parameters of the stereo sensor: camera models, inter camera situations, lens distortions... it allows computing the epipolar geometry between the cameras.

(a) (b) (c)

Figure 9: Some images: (a) empty seat, (b) child in a booster, (c) standing child

From on line acquisitions, the rectification process [6] corrects the original images, to perform a perfect virtual alignment of the two cameras and their epipolar lines; two matched pixels must be on the same line of the rectified images. Rectification and distorsion correction could require complex computations: these functions are performed in the same loop, using pre-computed tables to find the rectified $(u, v)$ coordinates from the real ones, and using simply a bilinear interpolation.

Then, for every line of the right and left images, the correlation process (figure 10) must match pixels, with respect to a similarity measurement based on windows centered on the compared pixels: several similarity measurements (SSD -Sum of Squared Differences-, ZNCC -Zero Normalized Cross Correlation-, CT -Census Transform-, ...) have been evaluated, using typically $11 \times 11$ windows. Every pixel $(u, v)$ on the left image, is compared to all potential matched pixels of the right image, located on the same $u$ line, from the position $v + d_{min}$ to $v + d_{max}$; a score function $score = f(d)$ is obtained, where $d$ is the disparity between the corresponding left and right pixels. A good optimum must be found from the *score* function. Several criteria can be used to filter false matchings: strength, uniqueness and form of the correlation peak (figure 11), and right-left validation. This last step inverses the role of left and right images and considers as valid only those matches for which the reverse correlation has fallen on the initial point in the left image [6].

Sub-pixel estimates are obtained by fitting a parabole to the correlation values surrounding the optimum. The quality is accessed not only by the correctness of the estimate, but also by the ability to filter out false matchings using the validity criteria.

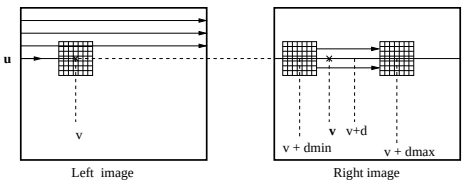


Figure 10: Left to Right correlation

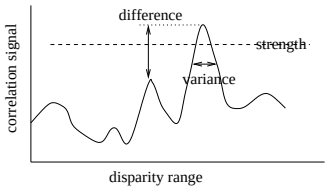


Figure 11: Detection of the correlation peak

The better similarity measurement has been selected in order to improve the robustness of the process with respect to environmental conditions; the CT score gives more matches, less artefacts in the disparity map and a better reconstruction than the classical scores. Nevertheless matching can be found only on textured areas of the images. On fig. 12, the disparity map is presented for an image of a pasenger in the cockpit: white points correspond to unmatched pixels, in homogeneous areas of the original image; generally, the correlation is very good on the passenger head or hands (skin, hair); CT score is better than ZNCC score.

At last the 3D reconstruction process based on triangulation techniques and on the calibration results, computes a depth map from the disparity map.

The performances of the stereovision method are good enough to fulfill real-time and accuracy requirements. The complete algorithm is executed in 250 $ms$ on $128 \times 128$ images; it provides a 3D dense reconstruction on the passenger seat (between 3000 and 5000 3D points) so that a large variety of situations (e.g. passenger in advanced or extended position, different objects, ...) could be sufficiently characterized to provide good inputs for a classifier. With such a frequency, the airbag requirements are not satisfied, especially for fast passenger motions (fast transition between safe and unsafe situations); the stereo frequency could be increased easily to 20Hz using a multi-resolution approach.

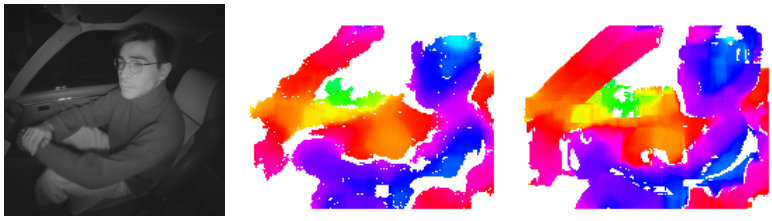

(a) (b) (c)

Figure 12: Stereo matching examples with a passenger on the seat: (a) original image, (b) disparity map with CT score, (c) disparity map with ZNCC score

## 3.2 Classification from stereovision

By now, the passenger seat classification is performed using a classical case-based approach. During a supervised learning step, a lot of prototypes are recorded for each class to be identified. The figure 9 presents some images of the large data base built in order to learn some characteristic configurations of the passenger seat. With respect to the NHTSA requirements concerning the firing conditions of the airbag, the work has been focused on identifying the following classes: (1) empty seat, (2) passenger in normal position, (3) passenger out of position, (4) empty booster, (5) child in a booster, (6) Front facing baby seat, (7) Rear facing baby seat, (8) object(s) on the seat.

The out-of-position configurations of a passenger (figure 3.2) are mainly

defined from the head position with respect to the airbag. Three areas are defined by two vertical planes parallel to the dashboard (figure 6); if some significative parts of the passenger are detected in the critical out-of-position area, then, the airbag cannot be inflated, while in the intermediate area, only a depovered inflation is desirable.

Figure 13: Out-of-position passengers

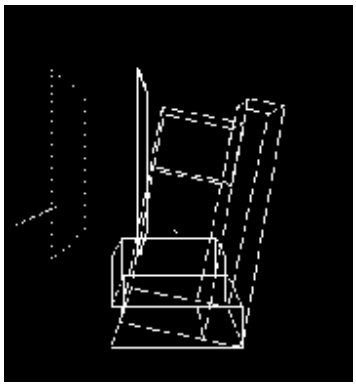

Figure 14: Pertinent areas in the cockpit

One difficult issue consists in identifying these situations without any false alarm or misclassification: the real time constraints are very severe, because the configuration changes could occur very fast (for example, a quick head motion in order to switch on the radio). A trade-off must be found between the computation time required by the data acquisition and analysis, against the classification capabilities of the system: with very few data processing, it is possible to detect the presence of something in the critical out-of-position area, but it is more than likely that mistakes or false alarms will occur.

The classification strategy uses a scene description as a set of local attributes (a specific detail located in a precise location: for example, number of points acquired in a given area of the cockpit, that could allow to identify a rear facing baby seat) or global ones (for example, number of points that belongs to planar faces, that could be significative to recognize an empty seat). These attributes must be *discriminant* (they must allow to distinguish between the classes), but also, *generic*, so that a generalization can be automatically obtained from the large learning data set, and *invariant* with respect to the possible modifications of the cockpit geometry, mainly the seat translation and the orientation of the seat back. This invariance issue is important, because all global attributes could fail, if they are not adapted with respect to the seat position and orientation.

An iterative method has been designed in order to find these seat parameters: from a initial position given by the lower point located in the left side of the 3D image and the higher point located in the right side, intermediate points belonging to the sitting or to the back part of the seat are integrated iteratively to the seat boundary, using some shape constraints that must be verified by

(a) (b) (c)

Figure 15: (a) Camera prototype, (b) vehicle integration, (c) cockpit representation

this boundary (maximum translation, maximum orientation, planarity...). The figure 17 shows the seat configuration for some images presented in figures 9 and 3.2.

Once this seat configuration has been computed, some specific areas are defined on figure 3.2: the segment on the left corresponds to the dashboard. The two security areas are limited by planes and five parallelipipedic boxes are defined on the seat to classify the passenger seat occupancy: two boxes for the seat volume (on the seat sitting and the seat back), one box above the sitting area and two boxes with variable heights along the seat back (the lower one for the passenger body, the higher one for the head). A preliminary classification, using as attributes, the number of 3D points which belong to these seven areas, gives good results, but it is not sufficient to deal with all possible configurations.

Within the context of passenger safety, the head plays a central role. Locating the head with respect to the dashboard is an important issue and fast, robust techniques need to be developed. Some segmentation methods have been explored based either on the density or the curvature estimate on each 3D point; such an approach could be performed only on a ROI corresponding to some boxes described here before. From the depth map, using a density criterion to extract the head when a passenger is detected, an accurate enough positioning of the head within the cockpit ($\simeq 2\ cm$) can be estimated.

### 3.3 Stereovision prototype

A low-cost and compact stereo head, developped for this application, consists in two synchronized low-cost sensor, mounted on the same board (figure 15-(a)). It integrates a wide angle NIR illuminator and shutter/gain can be controlled by means of a RS232 interface, with respect to the intensity computed in some areas of the images. Each sensor is equipped with a low-cost and compact optical lens (focal: 2.1 $mm$); such optic has high vignetting and distortion. In order to limit these drawbacks, only the central part of the images is processed; in this configuration, the perception field is bounded to a 110° view angle. On the figure 16, an image of the calibration pattern (located 25 $cm$ in front of the stereo head) shows clearly the importance of the calibration step required to correct the distortion in further processings.

This stereo prototype has been integrated in the cockpit of a demo car(figure 15-(b)). The different algorithms have been implemented in "C" code within a Windows NT environment; a dedicated Man-Machine-Interface allows to evaluate the method results(figure 15-(c)). First classification algorithms have been tested successfully (figure 17), but more intensive validations must be performed.

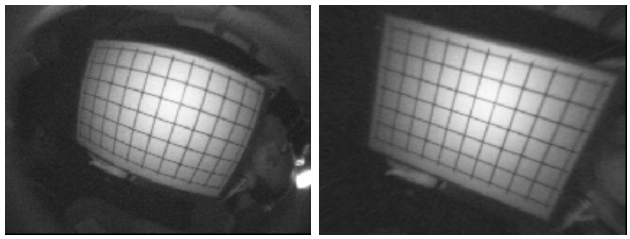

Figure 16: Distortion correction (2.1 $mm$ lens)

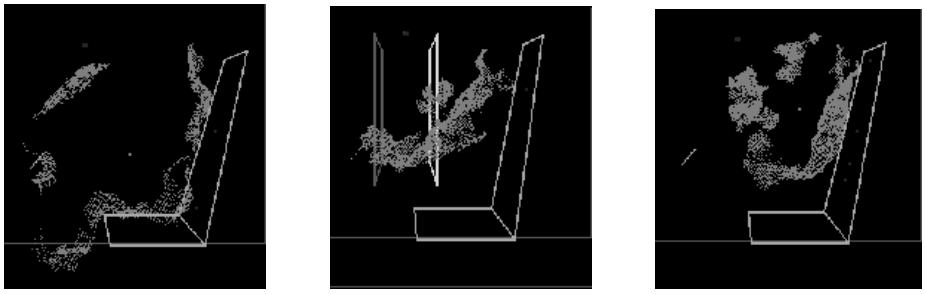

(a) (b) (c)

Figure 17: 3D points and seat configuration for images presented on figure 9

# 4 Comparison of the two approaches

3D vision based on structured light sensor shows some very good advantages for automotive application:

- The sensor can be realized in CMOS technology, cheap and high integrated solution can be viewed.
- First results show that 3D reconstruction using a restricted number of information allows a quite fast process with respect to the airbag requirements but some limitations exists in terms of resolution.
- Intensity images are still available and can be used for complementary processing.

- An homogeneous distribution of the light dots in the scene allows very good reconstruction capabilities.

Nevertheless some improvements must be brought concerning the compactness of the measurement device (camera + light emitter) and with respect to uncontrolled light disturbances and backlight.

Advantages of stereoscopic vision are mainly related with the very good resolution of the reconstructed image useful for classification purposes. In addition it is weakly influenced by backlights. As it consists in a passive system, eye safety requirements are not concerned with. Some remaining drawbacks concern the computation time and the non-homogeneous distribution of the reconstructed 3D image, so that it cannot be guaranteed that the field of interest will be always described.

# 5 Conclusion

New airbag generations will need more and more information about the automobile cockpit occupancy: nature of the occupant, distances to the dashboard... It is now obvious that 3D reconstruction of the cockpit inner space is necessary. Uses of video sensing for extracting this information look to be one of the real potential solutions. This technology is supported by the drastic reduction of the sensor cost but also by the exponential improvement and cost reduction of the image processing hardware. Within Siemens VDO Automotive, in collaboration with some labs and institutes, both in France and Germany, several video-based approaches have been evaluated for performing 3D reconstruction: conventional stereoscopic vision, 3D vision based on structured lightning, and time of flight techniques.

The results presented within this paper show the very high potentialities of the two first mentionned techniques. Beside the well known stereoscopic technique which gives a very high reliability of the reconstructed 3D images, but still remains slightly heavy in terms of computational time, uses of a structured light sensor looks to propose an interesting compromise between accuracy and speed. A combination of the two techniques should give optimal results: the presence of light dots on non textured areas should give 3D data where stereo by itself could not find points.

A strong interest of cars manufacturers, customers, governmental organizations has been identified for such 3D perception concepts. New "smart airbag" generation including partial inflation capabilities, should take into account information provided by such intelligent perception systems.

# References

[1] S. Boverie, M. Devy, J.M. Lequellec, P. Mengel, and D. Zittlau. 3D Perception for Vehicle Inner Space Monitoring. In *Advanced Microsystems for Automotive Applications*, pages 230–242, 2000.

[2] K.L. Boyer and A.C. Kak. Color-Encoded Structured Light for Rapid Active Ranging. *IEEE Trans. on Pattern Analysis and Machine Intelligence*, 9(31), 1987.

[3] M. Devy, V. Garric, and J.J. Orteu. Camera Calibration from Multiple Views of a 2D Object, using a Global non Linear Minimization Method. In *Int. Conf. on Intelligent Robots and Systems*, volume 3, pages 1583–1589, 1997.

[4] P. Faber and W. Forstner. A System Architecture for an Intelligent Airbag Deployment. In *IEEE Intelligent Vehicles Symp.(IV2000), Detroit (USA)*, 2000.

[5] S. Gautama, S. Lacroix, and M. Devy. On the Performance of Stereo Matching Algorithms. In *Erlangen Workshop : Vision, Modeling and Visualization*, 1999.

[6] P. Grandjean and P. Lasserre. Stereo vision improvements. In *Int. Conf. on Advanced Robotics*, volume 1, 1995.

[7] J. Krumm and G. Kirk. Video Occupant Detection for Airbag Deployment. In *Workshop on Applications of Computer Vision, IEEE Computer Soc.Press, Los Alamitos (USA)*, pages 30–35, 1998.

[8] J.M. Lequellec and F. Lerasle. Car Cockpit 3D Reconstruction by a Structured Light Sensor. In *IEEE Intelligent Vehicles Symp.*, pages 87–92, 2000.

[9] F. Lerasle, J.M. Lequellec, and M. Devy. Relaxation vs Maximal Cliques Search for Projected Beams Labeling in a Structured Light Sensor. In *Int. Conf. on Pattern Recognition*, volume 1, pages 782–785, 2000.

[10] L. Matthies and P. Grandjean. Stochastic Performance Modeling and Evaluation of Obstacle Detectability with Imaging Range Sensors. *IEEE Trans. Robotics and Automation*, 10(6):783–792, 1994.

[11] P. Mengel, G. Doemens, and L. Listl. Fast Range Imaging by CMOS Sensor Array through Multiple Double Short Time Integration. In *Int. Conf. on Image Processing*, pages 169–172, 2001.

[12] J.P. Rosenfeld and C.J. Tsikos. High-speed Space Encoding Projector for 3D Imaging. In *Optics, Illumination and Image Sensing for Machine Vision*, pages 146–151, 1986.

[13] G. Stockman and G. Hu. 3D Surface Solution using Structured Light and Constraint Propagation. *IEEE Trans. on Pattern Analysis and Machine Intelligence*, 11(4):390–402, 1989.